PRAMANA — journal of physics

Vol. 78, No. 3
March 2012
pp. 469–474

Electronic structures of the F-terminated AlN nanoribbons

YU-LING SONG[1,2,*], DAO-BANG LU[2], BEN-LIANG CUI[2] and JIAN-MIN ZHANG[1]

[1]College of Physics and Information Technology, ShaanXi Normal University, Xian, ShaanXi 710062, China
[2]College of Physics and Electronic Engineering, Nanyang Normal University, Nanyang 473061, China
*Corresponding author. E-mail: dblu985@163.com

MS received 1 May 2011; accepted 14 October 2011

Abstract. Using the first-principles calculations, electronic properties for the F-terminated AlN nanoribbons with both zigzag and armchair edges are studied. The results show that both the zigzag and armchair AlN nanoribbons are semiconducting and nonmagnetic, and the indirect band gap of the zigzag AlN nanoribbons and the direct band gap of the armchair ones decrease monotonically with increasing ribbon width. In contrast, the F-terminated AlN nanoribbons have narrower band gaps than those of the H-terminated ones when the ribbons have the same bandwidth. The density-of-states (DOS) and local density-of-states (LDOS) analyses show that the top of the valence band for the F-terminated ribbons is mainly contributed by N atoms, while at the side of the conduction band, the total DOS is mainly contributed by Al atoms. The charge density contour analyses show that Al–F bond is ionic because the electronegativity of F atom is much stronger for F atom than for Al atom, while N–F bond is covalent because of the combined action of the stronger electronegativity and the smaller covalent radius.

Keywords. First principle; electronic property; band structure; F-terminated; AlN nanoribbon.

PACS No. 73.21.−b

1. Introduction

Electronic and magnetic properties of single-layer graphene have attracted much attention [1–6]. The single-layered III–V semiconductors, especially the group III nitrides, have been widely used in electronic devices because of their high thermal stability and their potential technological applications [7–9]. Nanoribbons have attracted increasing attention because of their novel geometries as well as the promising properties relating to, e.g., optics and nanoscale electronic devices. As an important member of group III nitrides, AlN is the largest band-gap semiconductor, which is perfect for the epitaxial growth of the GaN-based heterostructures due to its small lattice mismatch with GaN and its superior properties such as high thermostability and conductivity and reliable

dielectric properties. Hence is widely used in electronic industry. Due to the large ionicity of the Al–N bond, AlN nanoribbons (AlNNRs) possess novel properties which are different from graphene nanoribbons leading to new potential applications in optics and nanoscale electronic devices. The perfect and with Al or N vacant AlNNRs with H termination have been intensively studied using first principles calculations and obtained some useful results [9]. However, some theoretical studies show that the electronic properties of the nanomaterials can be modulated by the terminated F atom [10–12]. Up to now, there are no reports about the electronic properties of F-terminated AlNNRs.

In this paper, AlNNR with zigzag edge (ZAlNNR) and armchair edge (AAlNNR) terminated with F atoms have been investigated by using the first-principles projector-augmented wave (PAW) potential within the density function theory (DFT) framework under the generalized gradient approximation (GGA). The rest of the paper is organized as follows. The calculation method and models of the two types of F-terminated AlNNRs are given in §2. The energy band structures, the density-of-states (DOS) and the charge density of the systems are analysed in §3 and conclusions are presented in §4.

2. Calculation method and structure model

The calculations are performed using the VASP based on DFT [13–18]. The electron-ion core interaction is represented by the PAW potentials [19]. To treat electron exchange and correlation, we chose the Perdew–Burke–Ernzerhof (PBE) formulation of the GGA [20], which yields correct ground-state structure of the combined systems. The cut-off energy for the plane waves is chosen to be 450 eV. The $2s^2 2p^3$, $3s^2 3p^1$ and $2s^2 2p^5$ electrons are taken as the valence electrons for N, Al and F atoms, respectively. In order to simulate infinite long isolated nanoribbon, we use a supercell geometry where each plane is separated from its replica by 15 Å in both edge-to-edge and layer-to-layer directions. The sampled k points in the Brillouin zone are generated by the Monkhorst–Pack scheme [21] with Γ-centred grids. To avoid numerical instability due to level crossing and quasidegeneracy near the Fermi level, we use a method of Methfessel–Paxton first-order smearing with a width of 0.2 eV. Geometric structures of the AlNNRs are fully relaxed to minimize the total energy of the system until a precision of 10^{-4} is reached. The conjugate gradient minimization is used for the optimization of atom coordinates until the forces acting on each atom are smaller than 0.02 eV/Å.

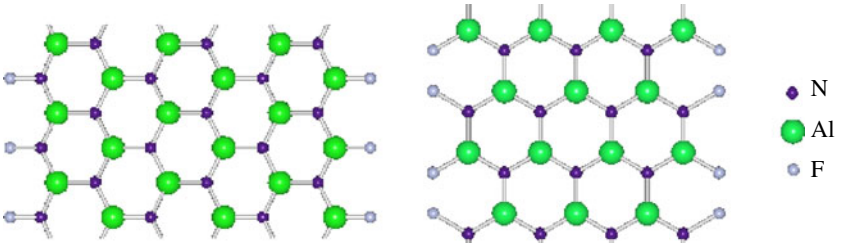

Figure 1. Geometry for (**a**) F-terminated 6-ZAlNNR and (**b**) F-terminated 7-AAlNNR.

The hexagonal network of AlNNR consists of alternating N and Al atoms with each N atom having three Al atoms as its nearest neighbours and vice versa. By following the convention used in nomenclature for GNR [7], the width of ZAlNNR is classified by the number of the zigzag chains (N_z) across the ribbon width and the width of AAlNNR is classified by the number of dimer lines (N_a) across the ribbon width. Thus we refer a ZAlNNR with N_z chains as N_z-ZAlNNR and an AAlNNR with N_a dimer lines as N_a-AAlNNR. Figure 1 presents the geometry for (a) 6-ZAlNNR and (b) 7-AAlNNR with F atoms termination. The purple, green and gray balls represent N, Al and F atoms, respectively.

3. Results and discussions

After geometry optimization, the average Al–N, Al–F and N–F bond lengths of the F-terminated AlNNRs is 1.83, 1.65 and 1.45 Å, respectively. Compared with the average Al–N, Al–H and N–H bond lengths 1.83, 1.60 and 1.02 of the H-terminated AlNNRs [9], the average bond lengths related to F atoms for the F-terminated AlNNRs increase more or less, and the average Al–N bond lengths have not been affected by the terminated F atoms. The covalent radius 0.37 Å of the H atom is much smaller than that of 0.72 Å of F atom which results in smaller average bond lengths for Al–H and N–H than those for Al–F and N–F, even though electronegativity of H atom is smaller than that of the F atom.

The band structures are presented in figure 2 and the total density-of-states (DOS) as well as local density-of-states (LDOS) are presented in figure 3 for (a) 6-ZAlNNR and (b) 7-AAlNNR. The Fermi level E_F is indicated by the black dashed lines. It is noted that either 6-ZAlNNR or 7-AAlNNR is semiconductor and nonmagnetic. The 6-ZAlNNR has

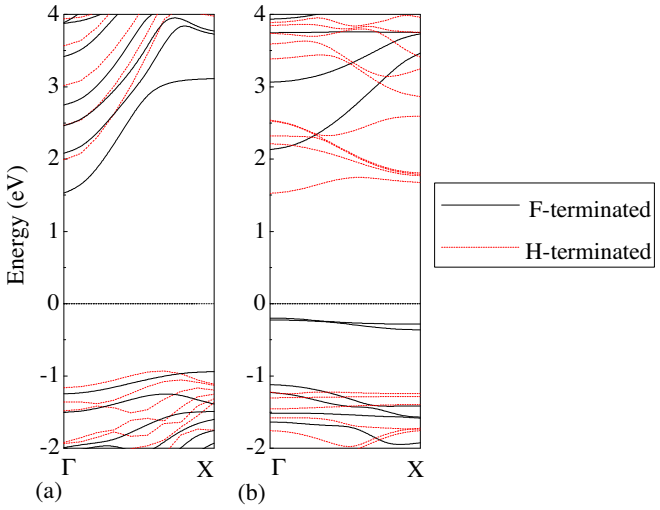

Figure 2. Band structures for (**a**) 6-ZAlNNR and (**b**) 7-AAlNNR. The red dashed and the black solid lines represent respectively the H- and the F-terminated AlNNRs. The Fermi level is set to zero and indicated by the black dashed line.

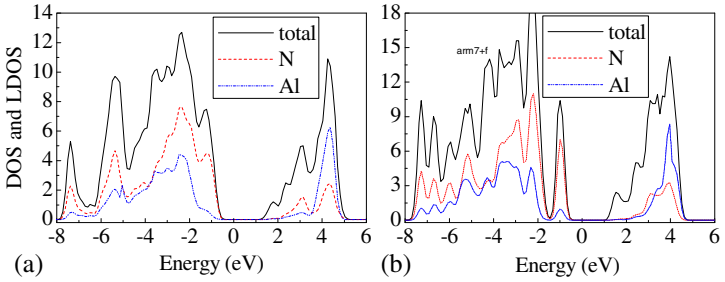

Figure 3. The total DOS and LDOS for (**a**) 6-ZAlNNR and (**b**) 7-AlNNR.

an indirect band gap of 2.4693 V, whereas 7-AAlNNR has a direct band gap of 2.3334 eV. This is analogous to AlNNR with H termination but different from GNR which can be metallic or semiconductor depending on their edge shapes [7,22]. Furthermore, the total density-of-states (DOS) at the top of the valence band is mainly contributed by the N atoms, while at the side of the conduction band, the total DOS is mainly contributed by the Al atoms.

In order to study the variation of energy gaps with ribbon width, in figures 4a and b, we present the variation of band gap as a function of the ribbon width for F- and H-terminated ZAlNNRs and AAlNNRs with the ribbon width up to 19. Distinct variation behaviours are exhibited with increasing ribbon width N_z for ZAlNNRs and N_a for AAlNNRs. It can be clearly seen that by increasing the ribbon width and thus decreasing the interaction between the two edges, band gaps of both ZAlNNRs and AAlNNRs decrease monotonically, irrespective of whether the termination is H or F. Moreover, it is more interesting that the F-terminated AlNNRs have narrower band gaps than those of the H-terminated ones when the AlNNRs have the same bandwidth. That is to say that, compared with the band gaps of the H-terminated AlNNRs, the band gaps of the F-terminated AlNNRs can be modified by F termination at both the edges of the nanoribbons. That is because of the σ–π mixing effect, that is, the non-bonding $2p$ electrons of F atoms produce an important orbital mixing with the s valence electrons [11,12]. This phenomenon is found in Si halide nanowires [10].

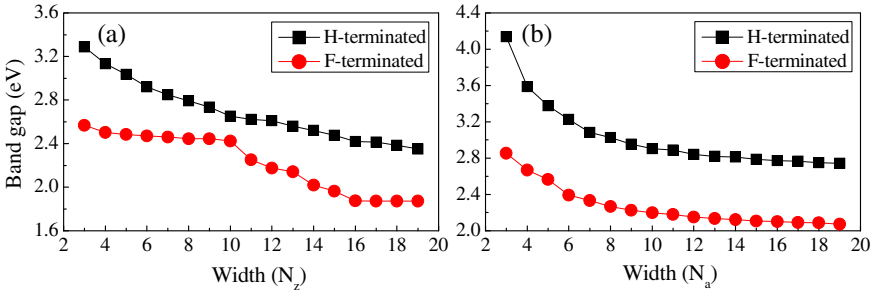

Figure 4. Variation of band gap as a function of the ribbon width for (**a**) ZAlNNR and (**b**) AAlNNR. (■) H-terminated, (●) F-terminated.

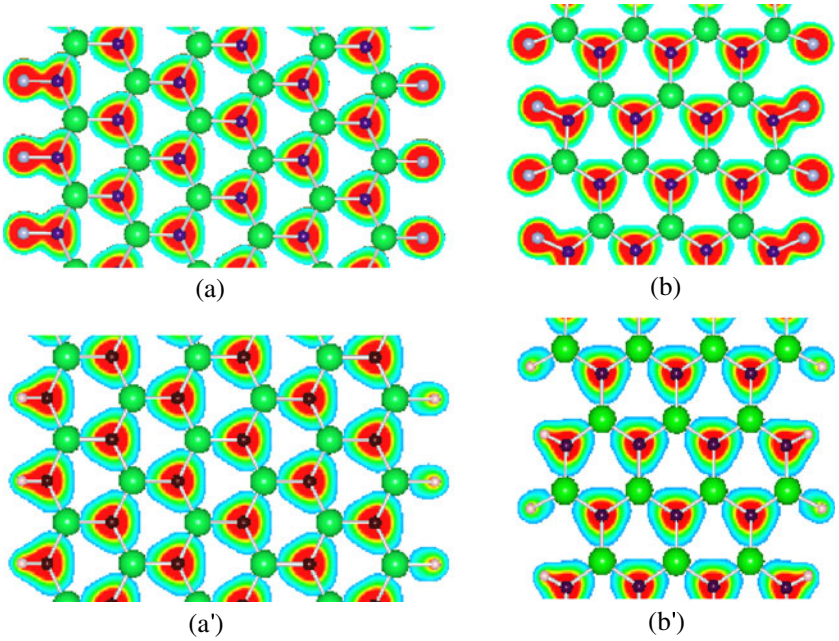

Figure 5. The charge density contours of (**a**) 6-ZAlNNR and (**b**) 7-AAlNNR terminated with F atoms as well as (**a′**) 6-ZAlNNR and (**b′**) 7-AAlNNR terminated with H atoms.

As examples, figure 5 presents the charge density contours of (a) 6-ZAlNNR and (b) 7-AAlNNR terminated with the F atoms as well as (a′) 6-ZAlNNR and (b′) 7-AAlNNR terminated with the H atoms. Because the electronegativity of N atoms is larger (3.04) than that of Al atoms (1.61), high-density contour plots around N atoms protrude towards the Al–N bonds indicating charge transfer from Al to N atoms. The large asymmetry in difference charge distribution displays a typical ionic bonding feature between Al and N atoms as in AlN [9] and BN [23]. Because the electronegativity is smaller (3.04) and the covalent radius is larger (0.75) for N atom than electronegativity (4) and covalent radius (0.72) for F atom, a typical covalent bonding resulted between the edge F atom and the nearest N atom. However, due to the much smaller electronegativity of Al atom (1.61) than that of the F atom, the Al–F bond displays a typical ionic bonding feature. Compared with the H-terminated ZAlNNRs, because of the smaller electronegativity (2.1) and the covalent radius (0.37) of H atom, the charge density plots around the H-terminated atoms are weaker than that around the F-terminated atoms of ZAlNNRs. Furthermore, the F-terminated AAlNNRs are in the same situation as the F-terminated ZAlNNRs.

4. Conclusions

The structural and electronic properties of F-terminated AlNNRs with different widths have been studied using first principles method under GGA. The band gaps of both the

ZAlNNRs and AAlNNRs with F termination are smaller than those of the H-terminated AlNNRs when AlNNRs have the same ribbon width because of the $\sigma-\pi$ mixing effect. The DOS and LDOS analyses show that the top of the valence band for the F-terminated AlNNRs is mainly contributed by N atoms, while at the side of the conduction band, the total DOS is mainly contributed by Al atoms. The large asymmetry in charge distribution displays a typical ionic bonding feature between Al and N atoms as well as between Al and F atoms, while N–F bond displays a typical covalent bonding feature, which is the same situation as the H-terminated AlNNRs except that the charge transport is more to F atom because of its larger electronegativity. The results show that different terminations can affect the electronic properties of the AlNNRs, which therefore can be tuned by using different terminations. Considering the potential application of the AlNNR, the F-terminated AlNNR has a competitive advantage because of its narrower band gap compared to that of the H-terminated GNRs.

Acknowledgements

The authors would like to acknowledge the support from the Science and Technology Key Project of Henan Province, China (Grant No. 102102310349) and Henan Province Education Department Natural Science Research Project, China (Grant No. 2011B510014).

References

[1] L Brey and H A Fertig, *Phys. Rev.* **B73**, 235411 (2006)
[2] Y W Son, M L Cohen and S G Louie, *Phys. Rev. Lett.* **97**, 216803 (2006)
[3] D A Abanin, P A Lee and L S Levitov, *Phys. Rev. Lett.* **96**, 176803 (2006)
[4] K I Sasaki, S Murakami and R Saito, *J. Phys. Soc. Jpn.* **75**, 074713 (2006)
[5] M Ezawa, *Phys. Rev.* **B73**, 045432 (2006)
[6] T Kawai, Y Miyamoto, O Sugino and Y Koga, *Phys. Rev.* **B62**, R16349 (2000)
[7] Z H Zhang and W L Guo, *Phys. Rev.* **B77**, 075403 (2008)
[8] A J Du, Z H Zhu, Y Chen, G Q Lu and Sean C Smith, *Chem. Phys. Lett.* **469**, 183 (2009)
[9] F L Zheng, J M Zhang, Y Zhang and V Ji, *Physica* **B405**, 3775 (2010)
[10] S Y You and Y Wang, *Chin. J. Semiconductors* **27**, 1927 (2006) (in Chinese)
[11] H Motoyama, K Takeda and K Shiraishi, *Proceedings of Materials Research Society Symposium* **486**, 385 (1998)
[12] D B Lu, Y L Song, Z X Yang and G Q Li, *Appl. Surf. Sci.* **256**, 6313 (2010)
[13] G Kresse and J Hafner, *Phys. Rev.* **B47**, 558 (1993)
[14] G Kresse and J Hafner, *Phys. Rev.* **B49**, 14251 (1994)
[15] G Kresse and J Furthmüller, *Comput. Mater. Sci.* **6**, 15 (1996)
[16] G Kresse and J Furthmüller, *Phys. Rev.* **B54**, 11169 (1996)
[17] H J Monkhorst and J D Pack, *Phys. Rev.* **B13**, 5390 (1976)
[18] W Kohn and L Sham, *Phys. Rev.* **A140**, 1133 (1965)
[19] G Kresse and D Joubert, *Phys. Rev.* **B59**, 1758 (1999)
[20] J P Perdew, S Burke and M Ernzerhof, *Phys. Rev. Lett.* **77**, 3865 (1996)
[21] H J Monkhorst and J D Pack, *Phys. Rev.* **B13**, 5188 (1976)
[22] Y W Son, M L Cohen and S G Louie, *Phys. Rev. Lett.* **97**, 216803 (2006)
[23] G Kim, B W Jeong and J Ihm, *Appl. Phys. Lett.* **88**, 193107 (2006)